MEASUREMENT OF VIBROTACTILE THRESHOLDS OF THE NON-PACINIAN I CHANNEL

by

Özge Kalkancı

B.S., Electronics and Communication Engineering
Istanbul Technical University, 2000

Submitted to the Institute of Biomedical Engineering in
partial fulfillment of the requirements for the degree of
Master of Science
in
Biomedical Engineering

Boğaziçi University
September, 2005

MEASUREMENT OF VIBROTACTILE THRESHOLDS OF THE NON-PACINIAN I CHANNEL

APPROVED BY:

Assist. Prof. Dr. Burak Güçlü ……..
(Thesis Supervisor)

Assist. Prof. Dr. Murat Gülsoy ……....

Assist. Prof. Dr. Can Yücesoy ……....

DATE OF APPROVAL: 20.09.2005

ACKNOWLEDGMENTS

I am greatly thankful to Assist. Prof. Dr. Burak Güçlü, for his supervising, guidance and consultancy during my thesis work.

I would also like to thank to Prof. Dr. İnci Çilesiz, whose motivation, inspiration and support made me accomplish this work.

I wish to thank Assist. Prof. Dr. Murat Gülsoy for his encouragement, support and helpful guidancy.

I would like to thank Assist. Prof. Can Yücesoy for being a member of my thesis committee and his valuable suggestions.

I am deeply grateful to the subjects of my experiments for their patience and great support.

This thesis is dedicated to my family. I am very grateful to them especially to my sister, Başak Kalkancı whose help, support and encouragement made this work possible.

ABSTRACT

MEASUREMENT OF VIBROTACTILE THRESHOLDS OF THE NON-PACINIAN I CHANNEL

The aim of this study is to measure the thresholds of the Non-Pacinian I (NP I) channel which is believed to be mediated by rapidly-adapting (RA) fibers. Thresholds of the NP I channel were measured using a two-interval forced-choice paradigm, a technique independent of the subject's criterion. The experiments were performed using the terminal phalanx of the human middle finger with a 40-Hz vibratory stimulus, but without using a contactor surround in order to enable comparison with population models of mechanoreceptive fibers in the literature. Since the Pacinian (P) channel and NP I channel have similar vibrotactile thresholds at 40 Hz, a forward-masking procedure was used to elevate the thresholds of the P channel with respect to the NP I channel. By this procedure P channel can be perceptually masked using a 250-Hz stimulus presented prior to the 40-Hz test stimulus.

In this study the masking functions of subjects were found to be approximately linear on log-log axes and the threshold shifts were found to increase as the masking-stimulus levels increased which indicates that the vibrations are perceived by the subjects more difficultly. The results confirm that the masking procedure is reliable and the NP I channel can be selectively activated at 40 Hz. The results are compared and discussed in relation to previous studies.

The long-term objective of this research is to provide information for determining the thresholds of other psychophysical channels as well for the application of the same method in auditory and visual threshold measurements.

***Keywords*:** NP I channel, Rapidly-adapting fiber, Meissner corpuscle, Forward masking.

ÖZET

PACINIAN OLMAYAN I. DOKUNMA KANALININ TİTREŞİMSEL EŞİK DEĞERLERİNİN ÖLÇÜLMESİ

Bu çalışmanın amacı hızlı uyum sağlayan (RA) lifler tarafından düzenlendiğine inanılan Pacinian Olmayan I. Dokunma (NP I) kanalının titreşimsel eşik değerlerini ölçmektir. Non-Pacinian I (NP I) kanalının eşik değerleri deneğin yargısından bağımsız olarak ölçüm almayı sağlayan iki aralıklı zorlanmış seçim paradigması kullanılarak ölçülmüştür. Deneyler mekanik algılayıcıların literatürdeki populasyon modelleri ile kıyaslama yapmayı sağlaması açısından insan orta parmağının üst boğumunun orta noktasına kontaktor çevreleyicisi kullanılmadan 40 Hz 'lik titreşim uyarısı verilerek gerçekleştirilmiştir. Pacinian (P) kanalı ve NP I kanalı 40 Hz de benzer eşik değerlerine sahip olduklarından NP I kanalının eşik değerini P kanalının eşik değerinden yalıtmak için ön maskeleme tekniği kullanılmıştır. Bu teknikle P kanalı 40 Hz'lik test uyarısı öncesinde uygulanan 250 Hz'lik bir uyarı ile maskelenmektedir.

Bu çalışmada deneklerin maske fonksiyonlarının eksenler logaritmik olarak düzenlendiğinde yaklaşık doğrusal olduğu ve eşik değerlerinin maske uyarı seviyeleri yükseldikçe arttığı bulunmuştur. Bu durum titreşimlerin maske uyarı seviyeleri arttıkça denek tarafından daha zor algılandığını göstermektedir. Çalışmanın sonuçları maskeleme yönteminin güvenilir olduğunu ve NP I kanalının 40 Hz'de seçilerek aktif hale getirilebileceğini söylemektedir. Bulunan sonuçlar bu alanda daha önceden yapılmış çalışmalarla karşılaştırılmış ve yorumlanmıştır.

Bu araştırmanın uzun dönemdeki amacı diğer psikofiziksel kanalların eşik değerlerinin belirlenmesinde bilgi sağlamaktır. Ayrıca işitsel ve duyusal eşik değerlerinin ölçülmesinde bu çalışmadaki tekniğin kullanılması ve çalışmalar arasında karşılaştırmaların yapılması mümkündür.

Anahtar kelimeler: NP I Kanalı, Hızlı alışan lifler, Meissner cisimciği, ön maskeleme.

TABLE OF CONTENTS

LIST OF FIGURES

LIST OF TABLES

LIST OF SYMBOLS

d	Distance from the stimulus source.
r	Radius of stimulus contactor area.
F	Probability value in statistical test “ANOVA”.
P	Probability value in statistical test “t-test”.
R	Correlation coefficient in regresion which measures the strength of the association between X and Y.

LIST OF ABBREVIATIONS

PNS	Peripheral Nervous System
P	Pacinian
NP	Non Pacinian
RA	Rapidly Adapting
FA	Fast Adapting
SA	Slowly Adapting
RF	Receptive Field
PC	Pacinian Corpuscle
LVDT	Linear Variable Differential Transformer
LED	Light Emitting Diode
ANOVA	Analysis of Variance
S	Subject

1. INTRODUCTION

Tactile perceptions are derived from the information provided by mechanoreceptors innervating the skin, and in some cases, the subcutaneous tissues. Cutaneous mechanoreceptors are defined functionally: those elements of the peripheral nervous system (PNS) that are selectively responsive to nonnoxious mechanical stimulation of the skin. A mechanoreceptor is the end organ that actually transduces mechanical energy into electrochemical energy, thus forming a neural signal. Often, however, both the transducing element and the associated nerve fiber is referred to as a mechanoreceptor. The skin is innervated by sensory nerve fibers possesing distinct and specialized response properties. Furthermore each fiber is associated with a morphologically identified end organ. The specialized end organ structure contributes to the physiological properties of the fibers. These facts indicate that specificity of peripheral afferent fibers, rather than the pattern of activity across nonspecific fiber types, forms the basis of somesthetic perceptual qualities. However, most tactile perception involves activity across the various afferent fiber types.

The main purpose of this study is to measure the sensation threshold of the Non-Pacinian I (NP I) channel at 40 Hz, which is believed to be mediated by rapidly-adapting (RA) fibers [1]. Because the average thresholds of the NP I channel and the Pacinian (P) channel almost coincide at low stimulus frequencies (e.g., around 40 Hz), the P channel must be masked to activate the NP I channel at these lower frequencies [1, 2]. To achieve this goal, absolute thresholds at 40 and 250 Hz are measured initially. Another goal of my study is to compare the new data with the results of previous studies [3, 4].

2. THEORY

2.1. Skin Anatomy and The Physics of Cutaneous Stimulation

The skin is a highly complex living structure that incorporates not only the sensory receptors and nerve fibers, but also blood vessels, sweat glands, and other specialized components such as hair, hoofs, claws, and nails. Skin is classified into three types, each having its own complement of mechanoreceptors and internal structure: glabrous or hairless skin (typified by the skin of the palm), hairy skin and mucocutaneous skin, which borders the entrances to the body's interior. The diverse structure of these three types of skin imparts differences in their mechanical properties. Furthermore, these mechanical properties (e.g., elasticity, resilience, thickness, attachment to subcutaneous tissues, etc.) can vary substantially as a function of body locus, age, gender, and species [5, 6]. Because of this variability, stimulus specification and control at receptor level is more difficult to achieve than for senses of vision and hearing.

The skin is composed of an outer layer (epidermis) and an inner layer (Figure 2.1 and Figure 2.2). The dermis seperates the epidermis from the underlying muscular tisue, ligaments, and bone. Both the dermis and epidermis are formed by strata having specific characteristics. The epidermis consists of stratified squamous epithelial cells in various stages of differentiation. The outermost layer, stratum corneum, is composed of dead cell tissue of a tough, horny nature. Epidermal cells are made in the lowest layer, the stratum germinativum (or basal layer), and migrate outwardly, eventually reaching the stratum corneum where they die. The epidermis contains no blood supply. In the glabrous skin (Figure 2.1), the boundary between dermis and epidermis is not a smooth plane; rather, there are regions called dermal pegs where the dermis and epidermis interdigitate. The physics of this arrangement appears important in determining mechanoreceptor activation.

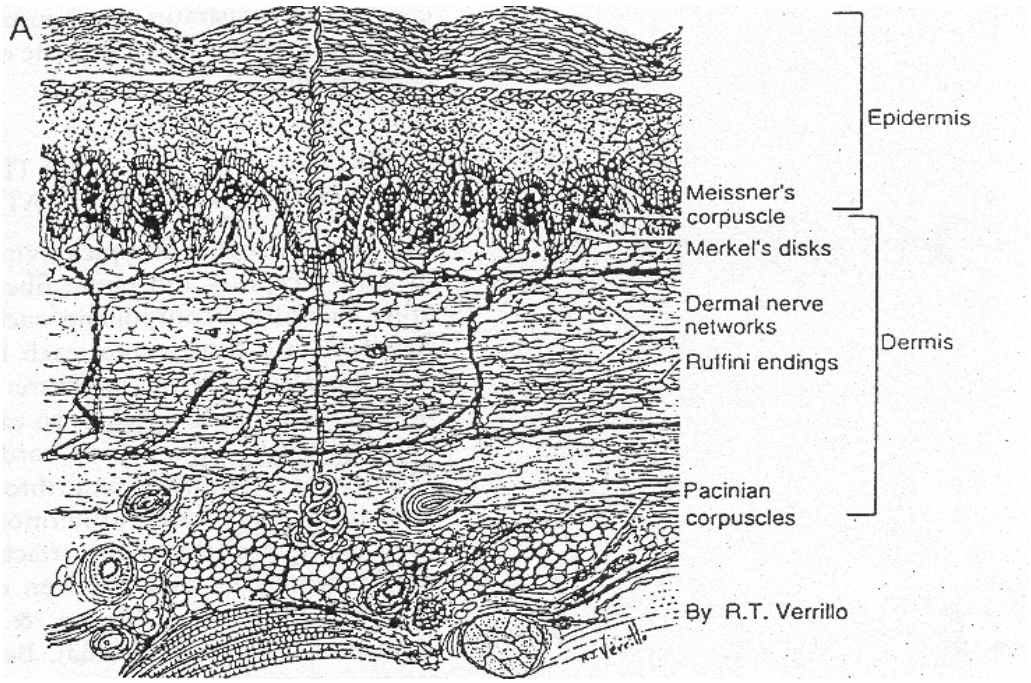

Figure 2.1 A Cross-section of glabrous skin [1]

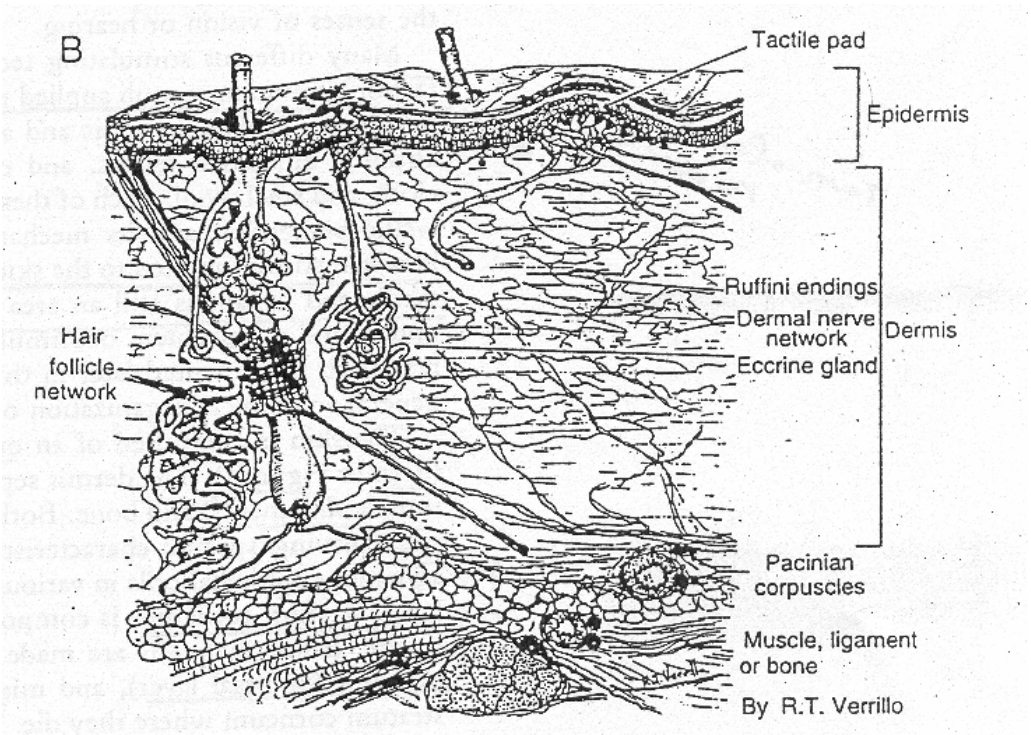

Figure 2.2 A Cross-section of hairy skin[1].

The dermis, in contrast, is composed of connective tissue and elastic fibers floating in a semi-fluid, nonfibrillary, and amorphous mixture called the ground substance. Also embedded in the ground substance are fat cells, blood vessels, the sensory receptors and the nerve fibers innervating them, smooth muscle, sweat glands, and a profuse blood and lymphatic supply. The dermis is composed of two layers, the papillary layer (prominent in humans) and the reticular layer. The papillary layer is composed of collagenous elastin and reticular fibers in a meshwork of capillaries, all of which is surrounded by ground substance. The reticular layer is composed of coarse collagen fiber bundles arranged parallel to the skin surface and loose networks of elastin fibers between the collagen, blood vessels, and nerve fibers. It also contains connective tissue cells (fibroblasts and mast cells), pigment-bearing cells, melanocytes, macrophages, lymphocytes, and leukocytes.

From a physical standpoint, the skin can be thought of as incompressible viscoelastic medium possessing the mechanical properties of viscous resistance (friction), stiffness (elastic restoring capabilities), and mass. Because of these properties, the skin has measurable mechanical impedance, which varies across skin type and body location. In considering the skin's physical response to mechanical stimuli, stresses (forces) and strains (deformations) occurring internal to the skin needs to be considered as well as those traveling across the skin. Within the skin, two kinds of internal waves are demonstrable: (a) the incompressible shear waves producing shear stresses and strains, and (b) irrotational compression waves producing normal stresses and strains. Normal strain, either perpendicular or parallel to the skin surface, is the adequate stimulus for transduction in tactile receptors. The actual strain transmitted through the skin surface is strongly dependent on the spatial structure of the stimulus. Assuming the incompressibility of the skin, displacements at the surface of the skin produce deformations within the skin that allow a $1/d^3$ relationship (d=distance from the stimulus source). Thus the strain is attenuated rapidly as the stimulus wave passes through the skin, and therefore is confined to the immediate vicinity of the stimulus [7, 8].

Traveling waves that propagate along the body surface from the point of stimulation are different from internal waves in several respects. The skin is a dispersive medium for surface waves, with increases in displacement frequency producing increases in the velocity of propagation of surface waves. Furthermore, the amplitude of surface waves decay in a manner proportional to the inverse square of the distance from the vibrating

stimulus. This decay is similarly dependent on stimulus frequency, in which higher frequencies result in greater decays for a given distance from the stimulus [9].

2.2 Mechanoreceptor Activation

Mechanoreceptors come in a variety of shapes and forms, and may or may not have nonneural elements attached or adjacent to the nerve terminations. The nonneural elements referred to as accessory structures, are thought to participate in selective filtering of mechanical stimuli, to allow for trophic influences, and to regulate the ionic environment around the nerve ending. One major class of endings with accessory structures is the encapsulated endings (Pacinian corpuscles, Ruffini capsules and Meissner corpuscles). The capsules of these receptors are organized in specific ways. For example, the Pacinian corpuscle has an onion-like layered arrangement and Ruffini capsule resembles a small muscle spindle. A second class of endings has accessory structures to which they are attached (Merkel cell-neurite complex, Iggo corpuscle). Another major class of endings in the skin is free nerve endings, which do not have accessory structures. This class of receptors is associated with transduction of thermal, or noxious (strong mechanical, thermal and/or chemical), or some types of tactile stimuli (i.e., C-mechanoreceptors) [10].

The mechanoreceptors' neural component typically consists of an unmyelinated nerve terminal continuous with a myelinated nerve fiber, which has its soma in the dorsal root. The unmyelinated nerve terminal is the region where mechanotransduction takes place, whereas the myelinated nerve fiber is capable of transmitting action potentials.

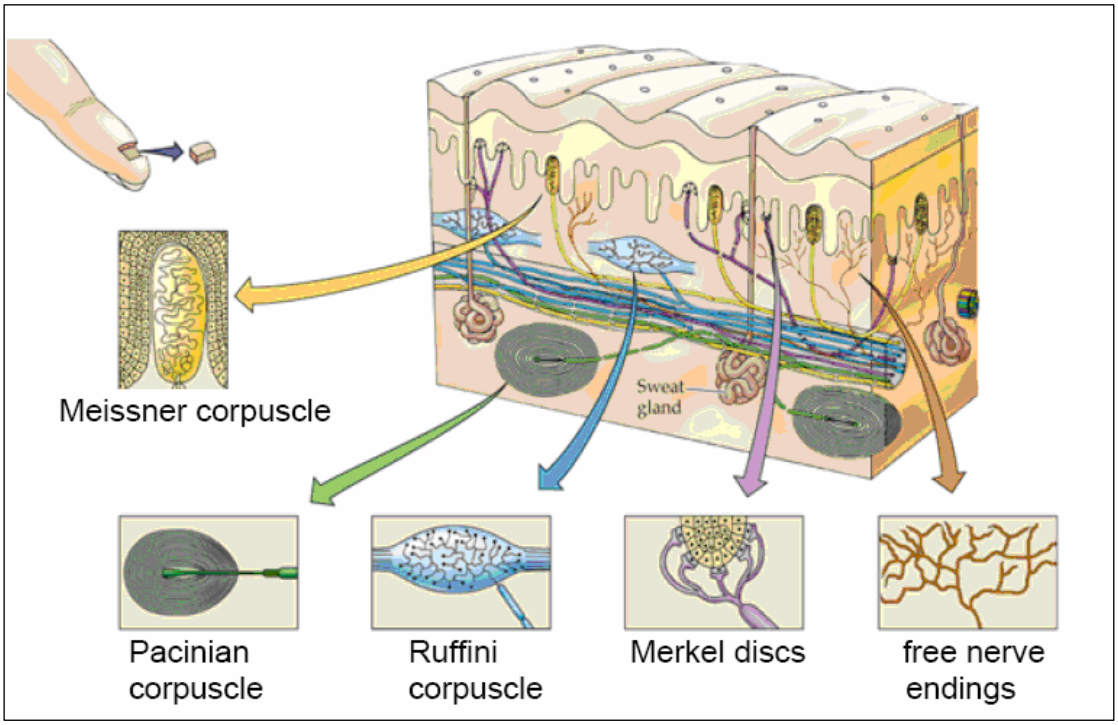

Figure 2.3 Mechanoreceptors in the glabrous skin [11].

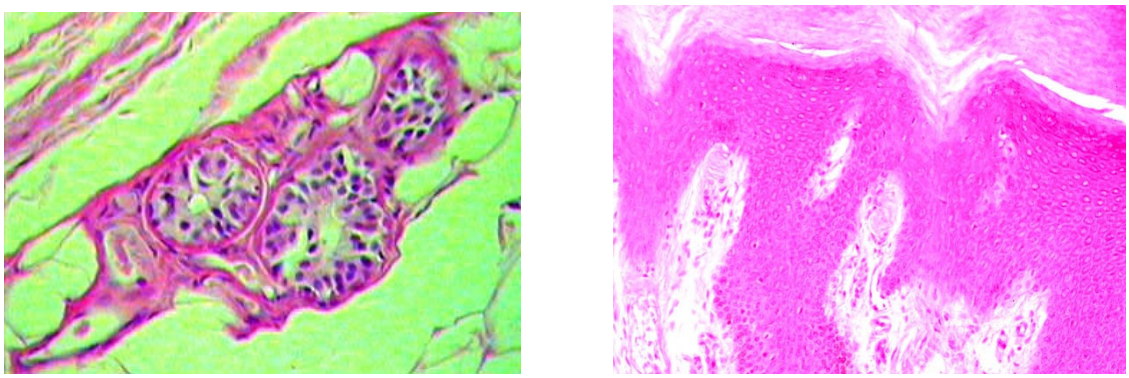

Figure 2.4 (A) Cross sectional image of Pacinian corpuscles, (B) Cross sectional image of Meissner corpuscles under microscope [11].

The manner in which cutaneously applied mechanical stimuli are transduced into electrochemical energy is not completely understood. One reason for this lack of knowledge is the receptors' inaccessibility for electrophysiological inverstigation while embedded in the skin. The transduction mechanisms of cutaneous mechanoreceptors has been derived primarily by studying Pacinian corpuscles. It is likely that the mechanisms of

transduction for the other tactile receptors are relevant to Pacinian corpuscle's transduction mechanism [10].

When a mechanical stimulus is applied to a Pacinian corpuscle, either through the skin or *in vitro*, the accessory capsule acts as a mechanical filter transmitting the applied strain to the transducing membrane. The strain induces stretch-sensitive channels to respond by increasing their conductance to certain ions, Na^+ in particular, and possibly K^+. This conductance increase produces the transmembrane event known as the receptor potential at a very short latency. Based on this short latency, the receptor potential cannot be mediated by neurotransmitters or other neuroactive substances potentially released by the surrounding accessory structure. If the receptor potential is sufficient enough in amplitude, an action potential will be generated and propagated along the peripheral axon to presynaptic endings within the central nervous system. Figure 2.5 shows levels of sensory information processing in the central nervous system. The receptor potential arises in the unmyelinated portion of the neurite specifically. The action potential originates near the unmyelinated-myelinated juncture. The specific location of the mechanoreceptive channels responsible for the receptor potential may be in the filopodia that extend from the unmyelinated nerve terminal. Filopodia are present on many dermal and epidermal endings [10].

In response to a ramp-and-hold stimulus, the Pacinian corpuscle's receptor potential first rises rapidly, and then decays. This phenomenon, called adaptation, is the basis for the rapidly adapting properties of the action-potential responses seen when recording form fibers innervating Pacinian corpuscles (Figure 2.6). The relationship between stimulus amplitude and magnitude of the receptor potential is linear at low-stimulus amplitudes and saturates at higher intensities. The greater the magnitude of the receptor potential, the greater the action potential firing rate. The mechanism for increased receptor potential magnitude with increased stimulus amplitude may involve a spatial sequestering of responses from discrete transduction sites operating in an all-or-none fashion. These transduction sites may be the filopodia and/or the putative strain-sensitive channels on the nerve ending [10].

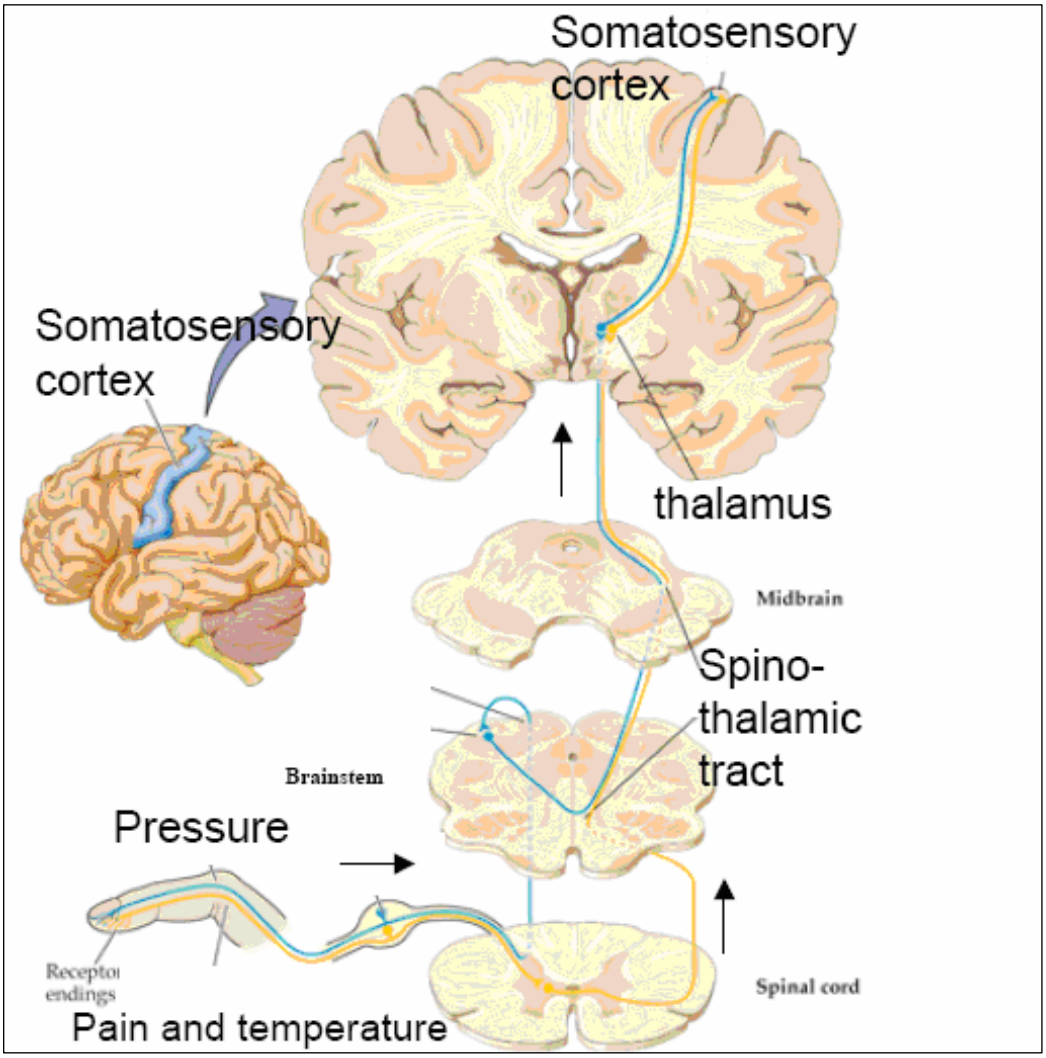

Figure 2.5 Levels of sensory processing in the central nervous system [11].

There are four types of mechanoreceptive afferent fibers innervating the glabrous skin of the human hand (Figure 2.6). There are two principle features that define these four types: adaptational properties and receptive field size. Two of these afferent types (i.e. SA I and SA II) are slowly adapting, whereas the other two–FAI (or RA) and FA II are fast (or rapidly) adapting. The "adaptation" in these cases refers to how these afferent fibers respond to a sustained skin indentation. FA afferents respond while the skin is actively being indented, but do not generate action potentials when the movement of the skin stops, even if the skin is still indented and under considerable force. SA afferents, in contrast, respond both while the skin is moving and during the period of sustained indentation.

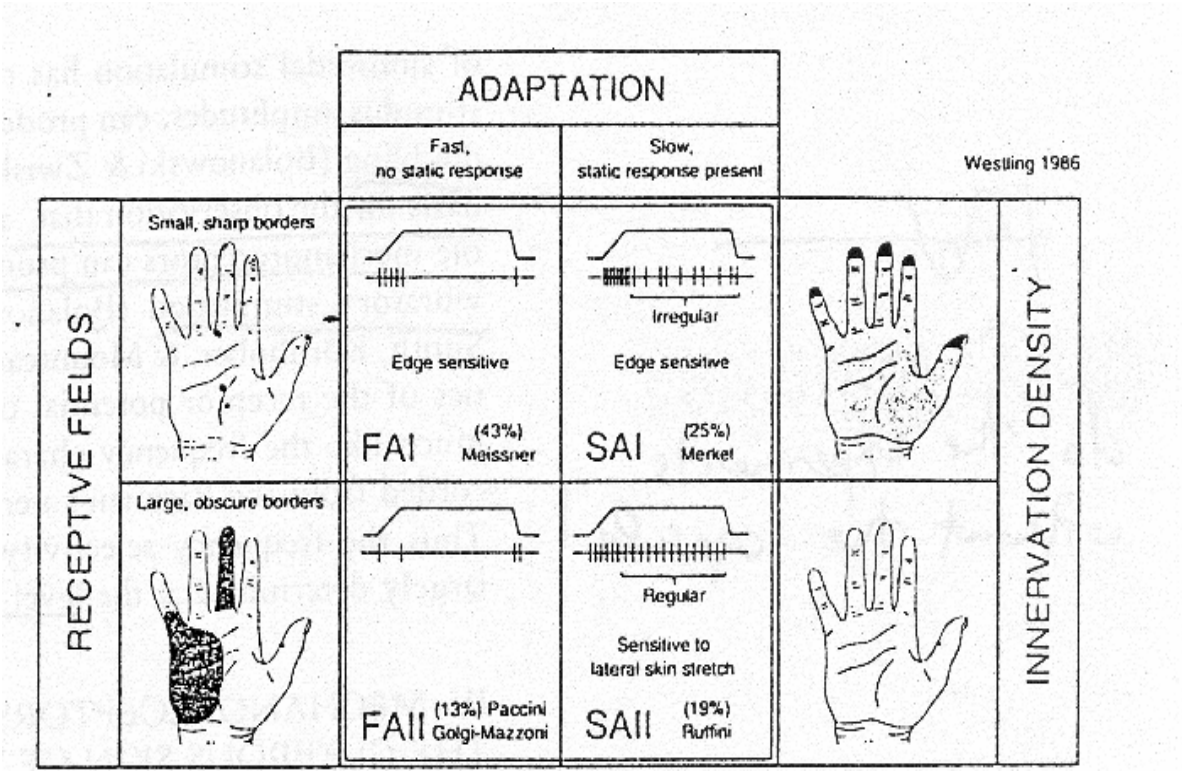

Figure 2.6 Characteristics of the four types of mechanoreceptive afferents that innervate the glabrous skin of the human hand. The center four panels show schematically the action potential discharges in response to a ramp-and-hold indentation of the skin. The center boxes also show the relative frequencies of occurrence of the four afferent types and the most likely morphological correlate. The black dots and the shaded areas of the hand figures on the left represent typical receptive fields of type I and type II afferents. The hand drawings on the right depict the average density of type I and type II afferents, in which darker areas indicate higher densities [10].

The receptive field (RF) of a mechanoreceptor is the area of skin that, when stimulated, will generate a response in that sensory neuron. The precise boundary of this area will depend on the intensity of the stimulus used. The type I fibers have smaller RFs than type II fibers.

Although adaptation and RF size are the defining characteristics of these afferent types, there are other distinguishing features. Each of these four afferent types has been identified with a specialized structure within the skin: the FAI (RA) afferent with the Meissner corpuscle, the FAII (PC) with the Pacinian corpuscle, the SAI with the Merkel cell-neurite complex, and the SAII with the Ruffini ending. Another aspect is the innervation density of these receptors within the hand. The type I afferents (FAI and SAI) exhibit a large gradient of innervations: The greatest density is found in the fingertips, becoming progressively more sparse in the proximal direction. The Type II afferents show only a slight difference in density across the hand [10].

3. PSYCHOPHYSICS OF TOUCH

Psychophysics is the scientific study of the relation between stimulus and sensation and therefore the problems of psychophysics constitute some of the most fundamental problems of modern psychology. The development of the theory of the signal detection and the refinements of methods for directly scaling sensory magnitude have greatly broadened the applicability of psychophysics to areas far beyond the original problems of measuring sensory thresholds. Modern psychophysics can be credited with contributions to the solution of problems in such diverse realms as sensory processes, memory, learning and social behavior.

Psychophysics serves two basic functions. One function is descriptive and involves the specification of sensory capacities; the other is analytical and involves testing of hypotheses about underlying biological mechanisms that determine sensory capacity [12]. In my experiment, the descriptive function of psychophysics will be the main focus in order to specify the sensory capacities in tactile perception.

Using vibratory (sinusoidal) stimuli in which the amplitude and frequency of displacements can be controlled independently and specified precisely, several investigators determined the sensory threshold at various frequencies for the glabrous skin of the human hand [13, 14].

There are four distinct psychophysical channels contributing to taction in the glabrous skin, each channel being mediated by a specific fiber type. The threshold-frequency characteristics of the four channels are determined by means of manipulating stimulus parameters, such as the frequency and the amplitude of vibration, probe or contactor size, stimulus duration and the application of various masking techniques [1].

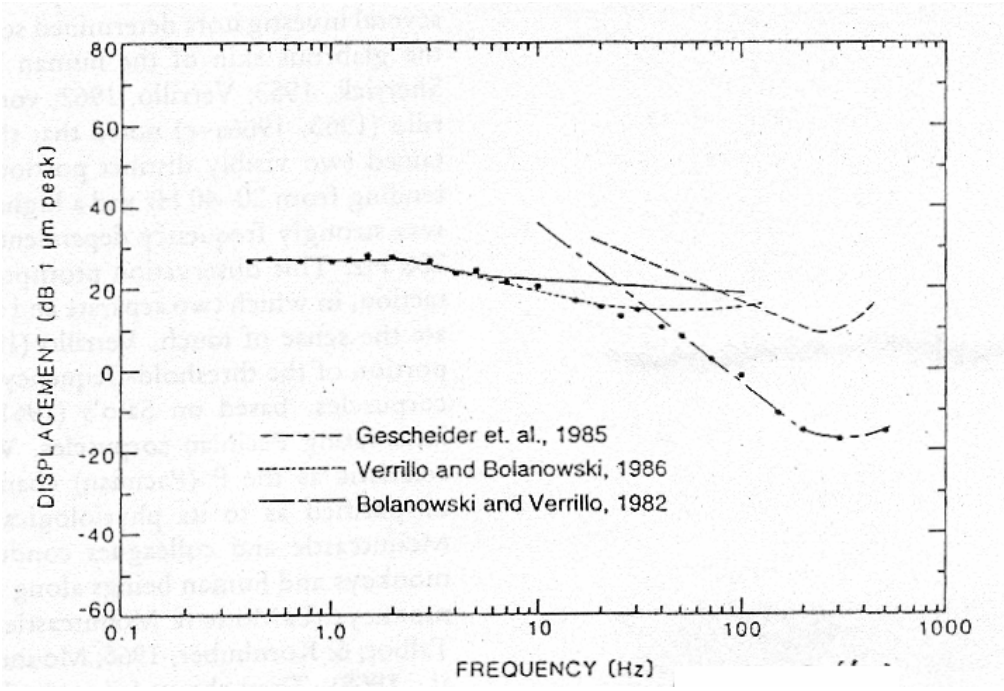

Figure 3.1 The four-channel model of vibrotaction showing the threshold-frequency characteristics of the various channels: —·—·—, P;·····, NP I;– – – –, NP II; and ————, NP III. Data points depict the psychophysically derived absolute thresholds for detection, as determined for thenar eminence using a 2.9- cm^2 stimulus area [1].

The four-channel model proposes that each psychophysical channel consists of specific end organs innervated by selected groups of peripheral nerve fibers, the isolated activation of which can produce unique unitary sensations and central neurons. Two major tenets of the model are that stimuli at threshold levels are signaled by the channel that is the most sensitive, and that suprathreshold sensations are the result of a combination of the neural activity transmitted by all activated channels.

The model also proposes these channels' end-organ-nerve-fiber substrates, their respective unitary sensations, and the nominal frequency range over which they operate at threshold levels are:

(a) P channel, mediated by Pacinian corpuscles and PC fibers, producing the sensation of "vibration" in the frequency range of 40-500 Hz.

(b) Non-Pacinian I (NP I) channel, mediated by Meissner corpuscles and RA fibers, producing the sensation of "flutter" in the frequency range of 2-40 Hz.

(c) Non-Pacinian II (NP II) channel, mediated by Ruffini end organs and SA Type II fibers, producing a buzz-like sensation in the frequency range of 100-500 Hz.

(d) Non-Pacinian III (NP III) channel, mediated by Merkel cell-neurite complexes and SA Type-I fibers producing the sensation of “pressure”in the frequency range of 0.4-2.0 Hz (Figure 3.1) [1].

4. METHOD

In my experiments, a contactor surround was not used in order to correlate the experimental results with theoretical studies on population models of mechanoreceptive fibers in the literature [15, 16, 17]. Using such a surround eliminates waves traveling on the skin, but also makes modeling more difficult. This is because the surround introduces an additional edge on the skin.

4.1 Subjects

Three male and two female healthy human subjects were tested. The subjects were required to be under 30 years of age, because it is known that the vibrotactile sensitivity decreases with age [18]. The terminal phalanx of the left or right middle finger was stimulated on the volar surface. The curvilinear distance from the joint line to the fingernail along the midline was measured before the experiment. The midpoint on this axis was marked with a felt-tip pen. The stimulus contactor probe was applied on this spot. The average surface temperature was not monitored during the experiment since the NP I channel is not temperature dependent [10].

4.2 Apparatus

The experiments were performed in a sound and vibration isolated booth. The stimuli were computer generated and amplified to drive a shaker. The shaker was mounted on a custom–made structure with a horizontal rail. The mechanical vibrations generated by the shaker were measured by a linear variable differential transformer (LVDT) and they were monitored on an oscilloscope. Block diagram of experimental setup, the pictures of the psychophysics laboratory that the experiments took place are shown in Figure 4.1 and Figure 4.2.

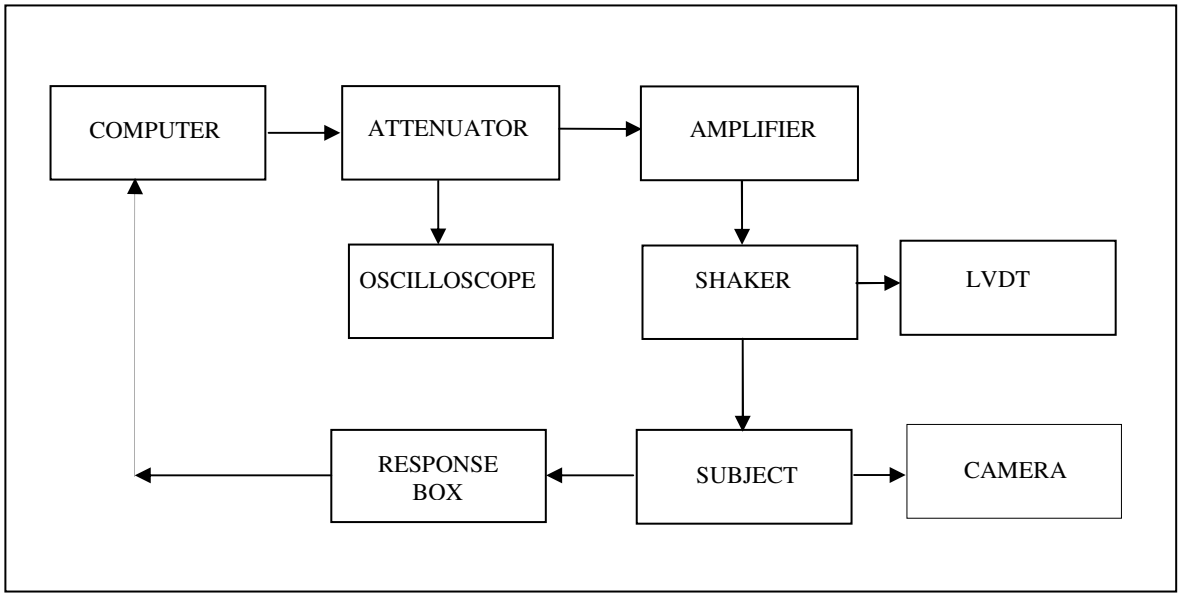

Figure 4.1 Block diagram of experimental setup.

The subject's middle finger was molded in modeling clay in order to prevent movement during the experiment. The fingertip was monitored by a camera mounted on the rail table and the experiment was halted in case of movement. This setup is shown in Figure 4.3.

The sound of the shaker that had been generated at high frequency vibrations was masked by continuous acoustic white noise presented to the subject on headphones. The response of the subject was obtained by a custom-made response box connected to the computer. The static indentation adjustment was made by a micrometer once the contactor tip had touched the skin. The initial contact was determined by measuring the resistance between the subject's body and the apparatus. The stimulus contactor area was 0.125 cm^2 (r = 2 mm).

(A) **(B)**

Figure 4.2 Psychophysics Laboratory (A) The picture of the booth as well as the experimental setup, (B) The outside of the booth.

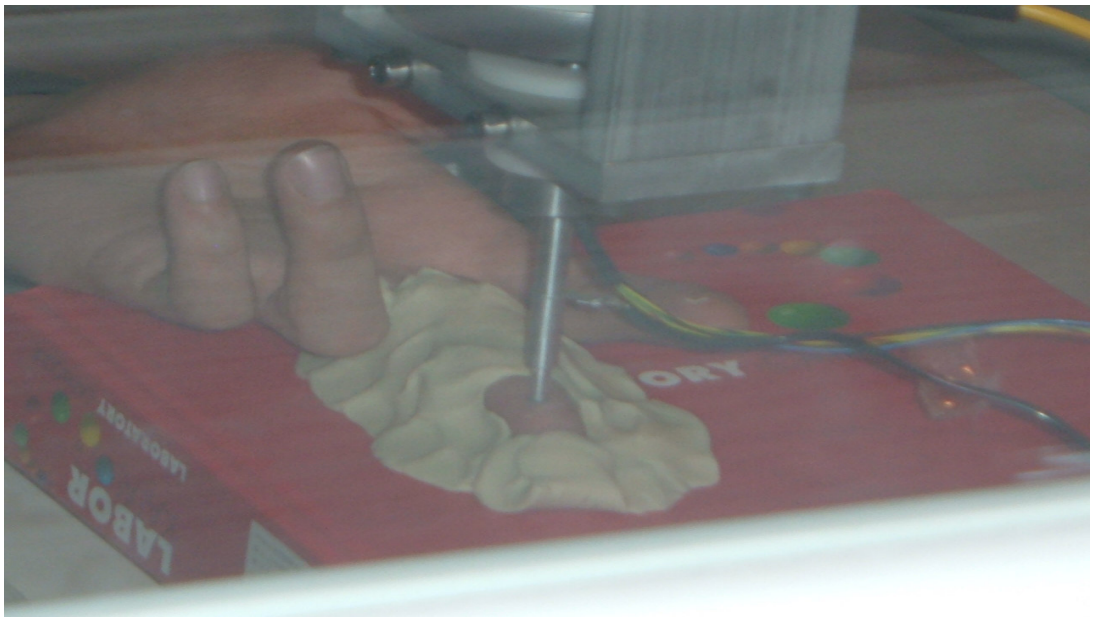

Figure 4.3 Subject's finger setup before the experiment.

4.3 Test and Masking Stimuli

The test stimuli were consisted of bursts of 40 Hz sine waves. The burst started and ended as cosine-squared ramps with 50-ms rise/fall times. Test stimuli had 0.5 s duration as measured at the half-power points (3 dB below peak displacement) of the burst. This duration is long enough to apply the time-dependent model developed for the responses of rapidly adapting (RA) fibers [17, 19].

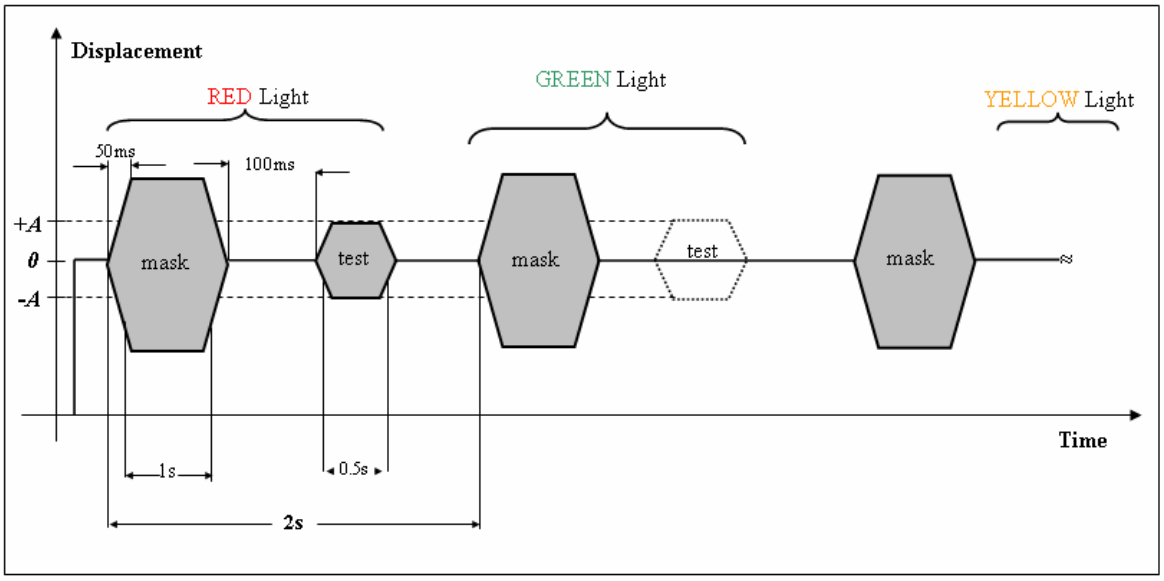

Figure 4.4 Stimulus timing diagram for the masked threshold measurement using the two- interval forced-choice task. Each interval begins with a high level masking vibration. The intervals are cued visually by red and green lights. The end of the trial is cued by another masking stimulus and the yellow light signals that a response from the subject is expected. The test stimuli (small burst, 0.5 s duration) occur randomly either in the first or the second interval inserted between the masking vibrations.

The stimuli were superimposed on a static indentation of 0.5 mm, in accordance with the previous physiological experiments and computational models. Maintaining the static indentation was important, since it was found that thresholds are affected by it [20].

Since the Pacinian (P) channel and Non Pacinian I (NP I) channel may have similar vibrotactile thresholds at 40 Hz, the P channel must be masked to ensure detection of the 40 Hz stimuli by the NP I channel [1]. A forward masking procedure with a 250-Hz masking stimulus was used to elevate the thresholds of the P channel with respect to the

NP I channel. The intensity of the masking stimulus was determined individually for each subject to generate adequate masking. The masking stimuli were sine bursts of 1 s duration and 50 ms rise/fall times. This duration was adequate to produce forward masking. The intervals between the masking stimuli were 2 s in each trial and each trial ended with a third masking stimulus. This arrangement made the placement of the test stimulus symmetric among the masking stimuli (Figure 4.4). The test stimuli were presented 100 ms after the masking stimulus. 100 ms was chosen because it was adequate for a robust masking effect [21].

4.4 Procedure

Sensory thresholds of NP I channel were measured using a two-interval forced-choice paradigm, a technique to measure sensitivity unaffected by the observer's response bias. In two-interval forced-choice procedure, the observer is given two observation intervals, one of which contains a signal in random. The observer is required to choose the observation interval which contains the signal. This method can produce results independent of the subject's response bias.

First absolute thresholds of each subject were measured. The stimulus levels were changed according to an up-down rule which tracks thresholds at 75 % correct detection probability [22]. This is an adaptive procedure, in which the sequence of correct and incorrect responses since the last change in the stimulus level determines the level of the next stimulus. The level of the test stimulus was increased by 1 dB for each incorrect answer and decreased by 1dB for three, not necessarily consecutive, correct answers. The tracking was stopped when the stimulus intensity was within +/ - 1dB of an intensity level for the last 20 trials. This intensity level was recorded as the absolute or masked threshold of the subject depending on the experiment. Then masking functions were determined for each subject. In order to measure the change in threshold during masking of the P channel, both the masking and the test stimuli were 250 Hz.

The intervals were cued visually by red and green light LEDs. The trial was ended with another masking vibration and the yellow light LED indicated a response from the subject was expected.

Each threshold measurement was repeated five times for each subject. Five suprathreshold intensity levels stimuli were tested in order to get masking functions for each subject. Each measurement took approximately five minutes.

4.5 Analysis

The graphs presented show the averages of the data collected. The graphical points are the averages of 5 experimental measurements taken from each subject. The error bars are sample standard deviations of measurements. Statistical tests (two-sample t-tests and ANOVA) were performed on absolute displacement values in dB in Microsoft Excel 97. The best-fit lines in Figures 5.5, 5.6, 5.7, 5.8, 5.9 are linear regression results.

5. RESULTS

5.1 Comparison with previous experiments

Figure 5.1, Figure 5.2 and Figure 5.3 show individual unmasked thresholds of 5 subjects in terms of dB re 1-um peak displacement amplitude for 40 and 250Hz . For 40Hz, the unmasked displacement thresholds for 5 subjects are shown in Table 5.1. For 250Hz the unmasked displacement thresholds for five subjects are shown in Table 5.2.

Table 5.1
Absolute displacement threshold values of each subject for 40Hz.
The absolute thresholds are found between 8 and 19 dB.

	ABSOLUTE THRESHOLD (dB)
S1	8.3
S2	14.7
S3	14.6
S4	16.6
S5	18.8

Table 5.2
Absolute displacement threshold values of each subject for 250Hz.
The absolute thresholds are found between -7 and -26 dB.

	ABSOLUTE THRESHOLD (dB)
S1	-14.3
S2	-11.9
S3	-26
S4	-11.6
S5	-7.1

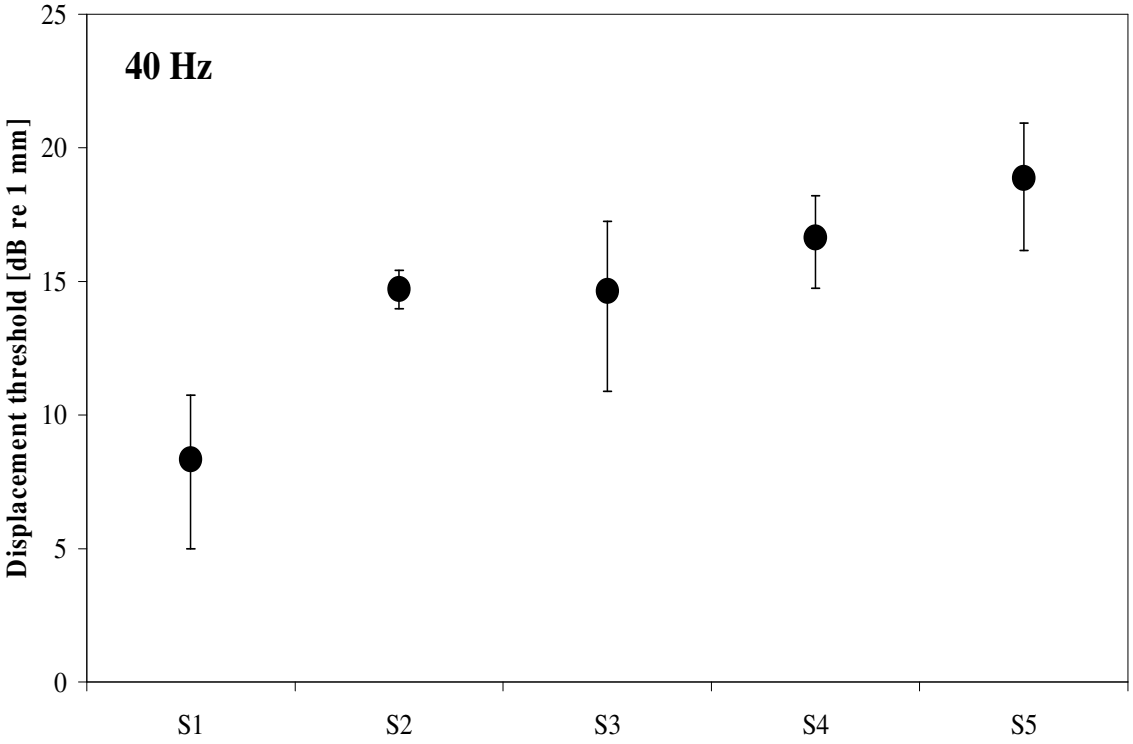

Figure 5.1 Unmasked thresholds at 40 Hz.

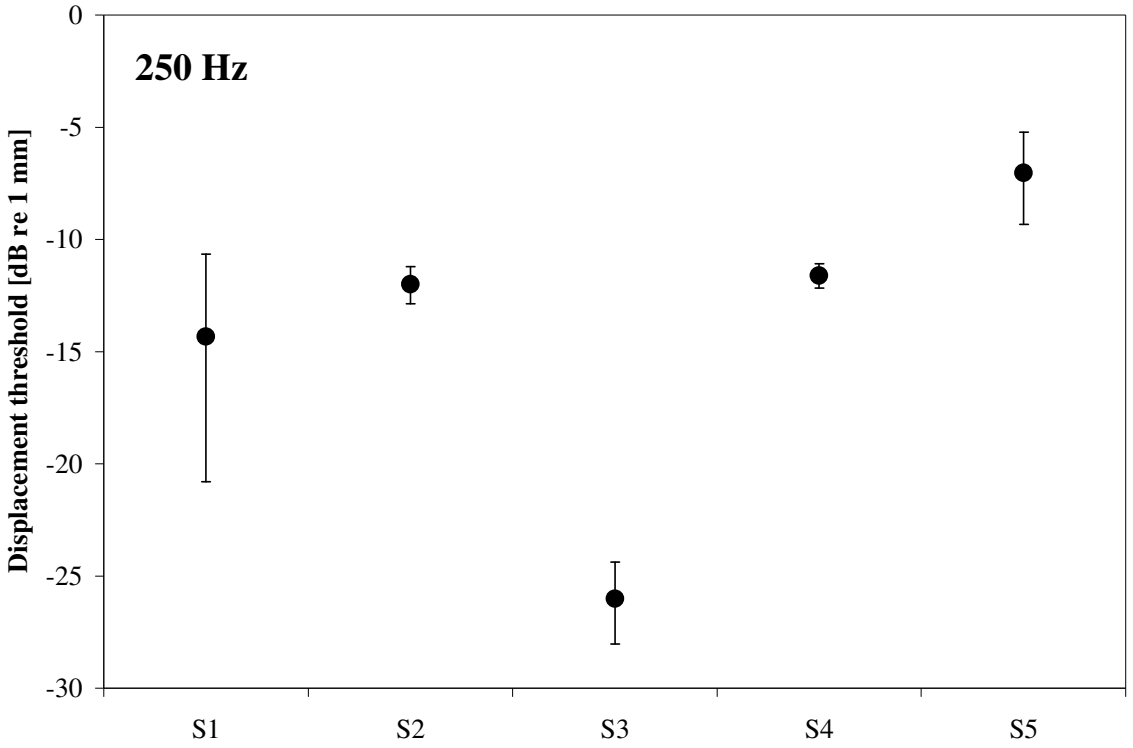

Figure 5.2 Unmasked thresholds at 250Hz.

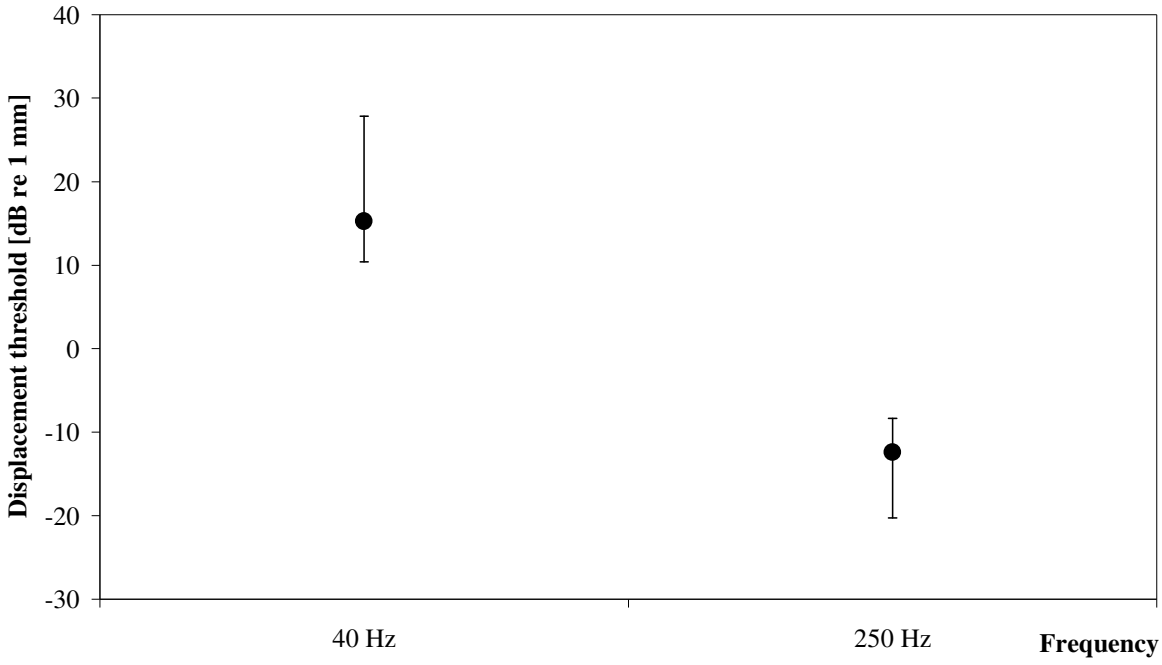

Figure 5.3 Averages of unmasked thresholds of all subjects.

To compare and determine the statistical significance for subject to subject variance of absolute threshold values at 40 and 250 Hz, statistical test "ANOVA" is run. The hypothesis is that averages from five subjects are equal or drawn from populations with the same average. Then on the basis of this hypothesis, ANOVA computes the value of a variable F; the larger the value of F, the more unlikely it is to have occurred by chance, and hence the more likely that at least one of the populations has an average different from the others. If F is not large enough, the conclusion is that all the populations have equal averages. So for 40 Hz, at significance level of 0.05, F=10.777 and the critical value of Fcrit=2.866. Since F> $F_{crit,}$ there is a significant difference between at least one pair of sample averages. For 250 Hz, at significance level of 0.05, F=409.509 and F_{crit}=2.866, like 40 Hz, since F> F_{crit}, it can be said that there is a significant difference between at least one pair of sample averages. As a conclusion, the average absolute thresholds vary across subject, both at 40 Hz and 250 Hz.

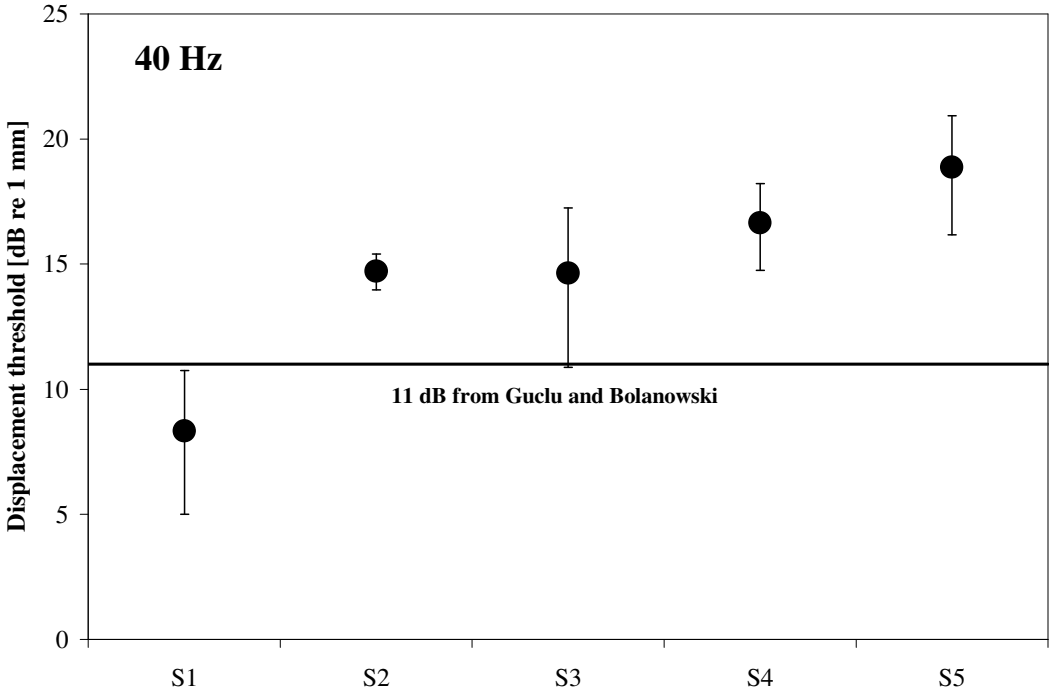

(A)

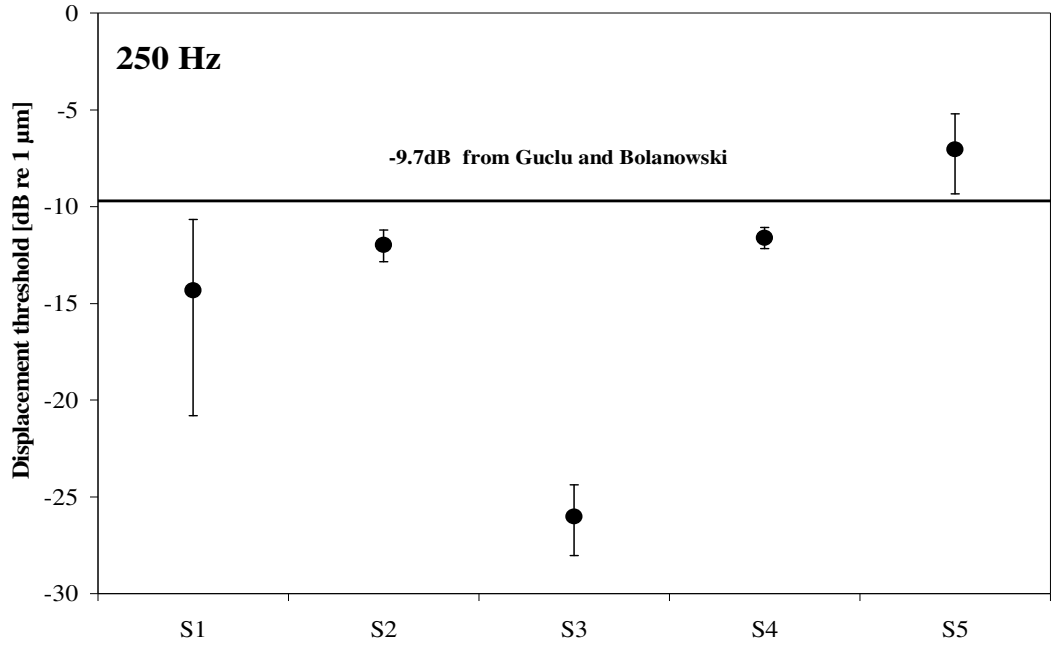

(B)

Figure 5.4 (A) Unmasked thresholds at 40 Hz found in my study are mostly higher than the average threshold in Güçlü and Bolanowski's] study [3]. (B) Thresholds at 250 Hz in my study are mostly lower than the average threshold in Güçlü and Bolanowski's [3] study.

The unmasked thresholds obtained for 40 and 250 Hz were compared to results of Güçlü and Bolanowski [3]. Figure 5.4 displays values from my study and the values found by Güçlü and Bolanowski [3] for 40 and 250 Hz.

To compare and determine the statistical significance between the thresholds of my study and Güçlü and Bolanowski's [3] study, two sample t-test was run. The null hypothesis for the two-sample t-test is that both of the thresholds in my study and in Güçlü and Bolanoswki's [3] study come from the same population. For 40 Hz, the P-value is 0.114 and for 250Hz the P-value is 0.230. According to the two-sample t-test since the P-values are higher than 0.05, the null hypothesis can not be rejected. This means that there is not sufficient evidence to conclude that the thresholds are significantly different. As a result, the unmasked thresholds of all subjects of my study and the unmasked thresholds of all subjects of Güçlü and Bolanowski's [3] study are not significantly different.

5.2 Masking the P Channel

The P-channel thresholds are elevated to various degrees for all 5 subjects. Figure 5.5, Figure 5.6, Figure 5.7, Figure 5.8 and Figure 5.9 show the masking functions for each subject.

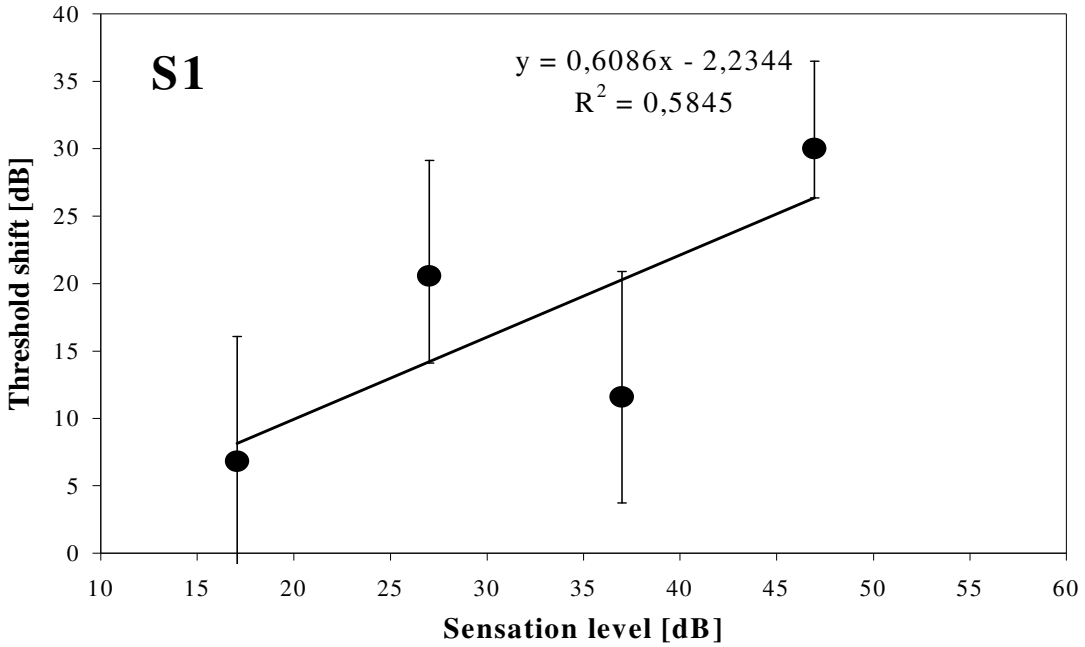

Figure 5.5 Masking function for S1.

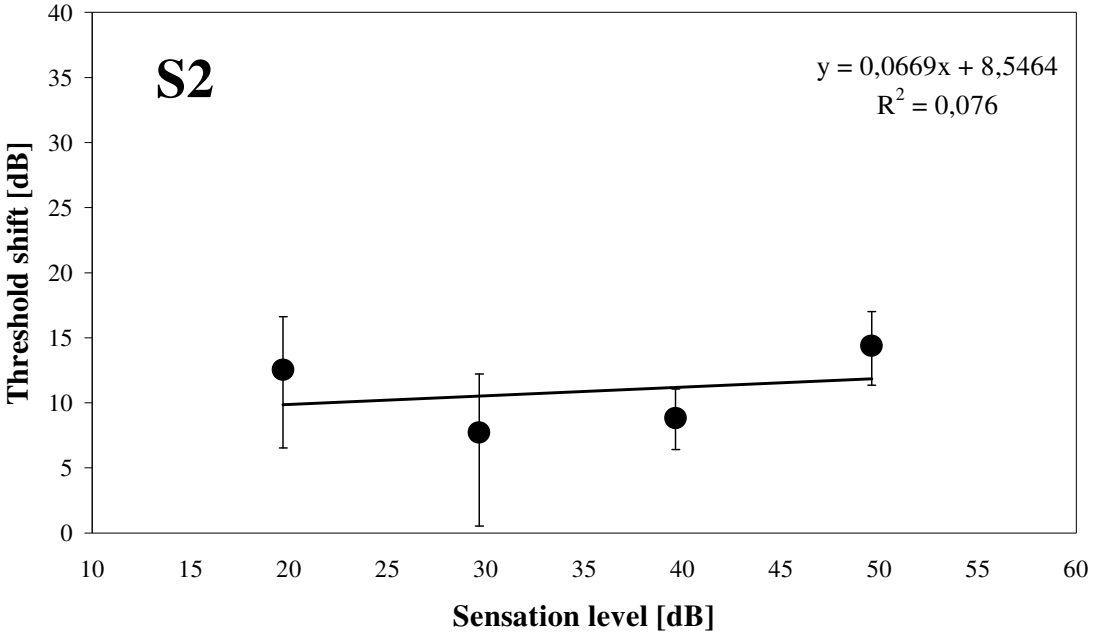

Figure 5.6 Masking function for S2.

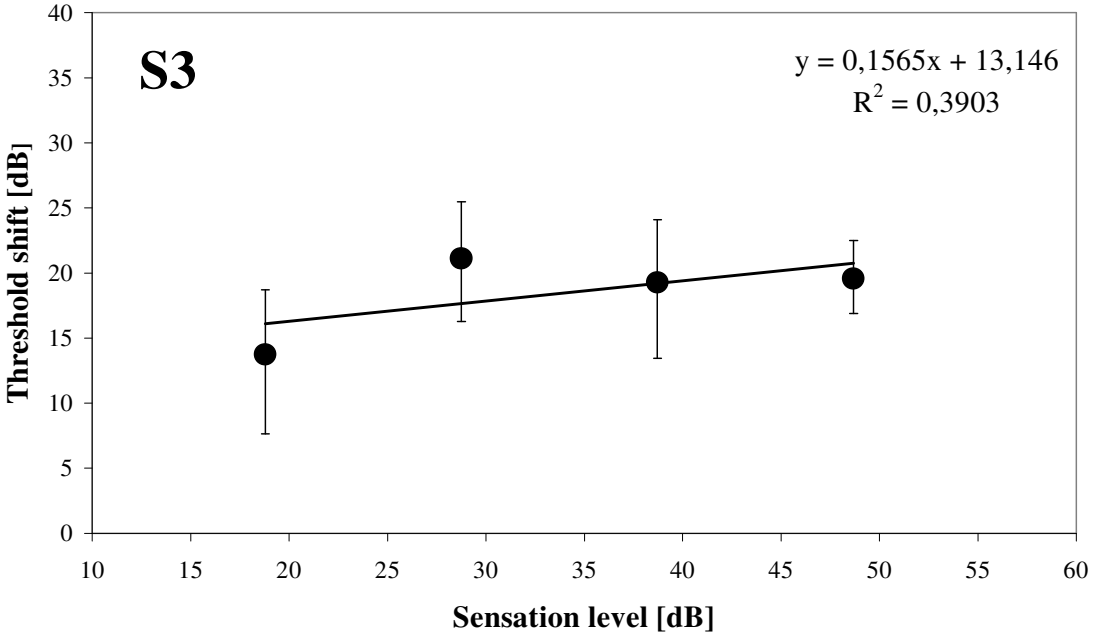

Figure 5.7 Masking function for S3.

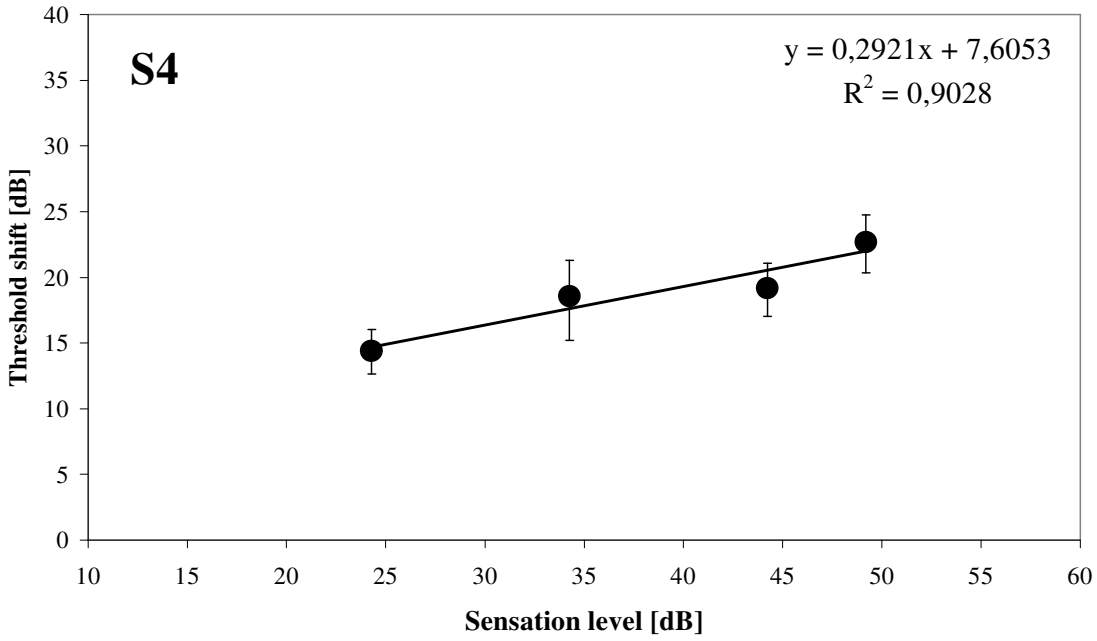

Figure 5.8 Masking function for S4.

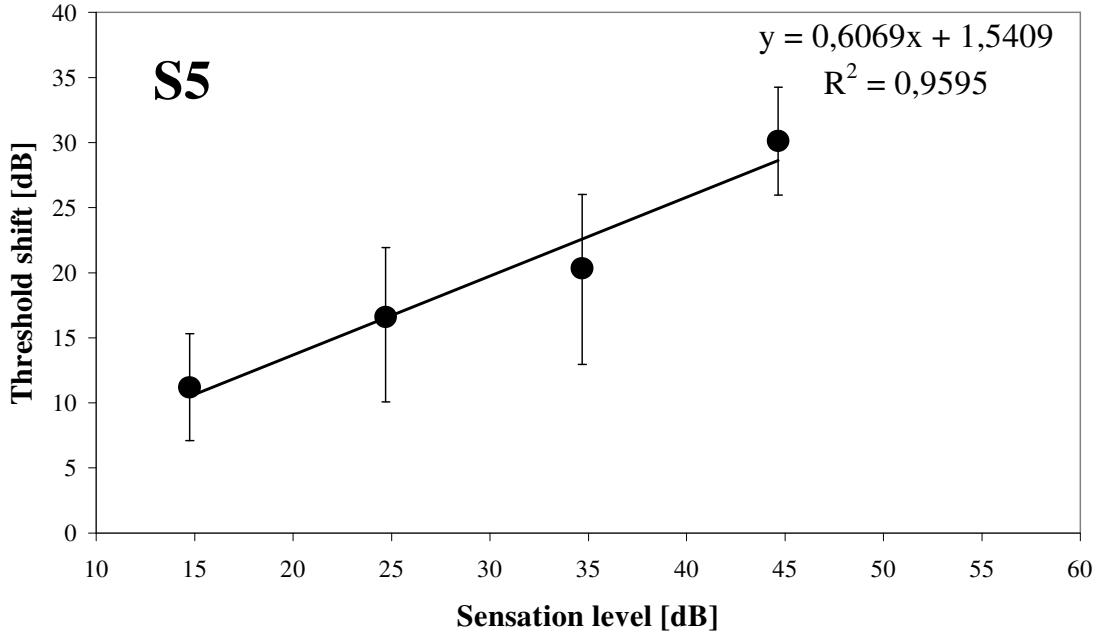

Figure 5.9 Masking function for S5.

In Figures 5.5, 5.6, 5.7, 5.8 and 5.9, the P channel was masked by a 250- Hz vibration. The graphs show the shift in the threshold for the detection of a 250-Hz stimulus with forward-masking. For a given threshold shift, the masking level required for each subject is different. The data points are averages of five measurements. Error bars are the standard errors of the mean. The linear regression results are given on each plot.

The threshold shifts which means the level of thresholds are plotted in dB values as a function of the level of masking in dB referenced to sensation level. These plots indicate the masking levels which are referenced to the unmasked thresholds of each subject at 250 Hz.

Since the masking functions for each subject are different, the masking levels and the masking effects obtained for each subject are different. For every subject different masking intensities were applied and looked for a noticeable decrease (like 10 dB) in subject's absolute threshold value at 40 Hz. The sensation levels determined for masking are 46.95 dB for S1, 49.6 dB for S2, 38.71 dB for S3, 34.26 dB for S4 and 24.7 dB for S5.

As the sensation levels increase, the thresholds measured at 250 Hz also increases. This indicates that the vibrations are perceived by the subjects more difficultly.

The masking intensity in the masking function plot at which the average 10-15 dB decrease of absolute threshold of the subject had been observed was selected. At this masking intensity the forward masking procedure was applied again. The masked thresholds at this specific masking intensity and unmasked thresholds were compared by using a two-sample t-test. P-values are smaller than 0.001 for S1 and S2, are equal to 0.021, 0.002 and 0.014 for S3, S4 and S5 consecutively.

The null hypothesis for the two sample t-tests is that the masked and unmasked thresholds at 40 Hz for each subject are coming from the same population. According to the two-sample t-test, since the P-values are lower than 0.05, the null hypothesis is rejected. As a result, the unmasked and masked thresholds for each subject are significantly different.

5.3 Detection Mechanism

At 40 Hz, the P and the NP I channels have the lowest thresholds; and since all tactile channels are assumed to be independent, at least peripherally, interactions of the remaining two channels need not be considered at threshold level [1]. There are two possible scenarios for the detection of 40 Hz stimulus [Figure 5.10].

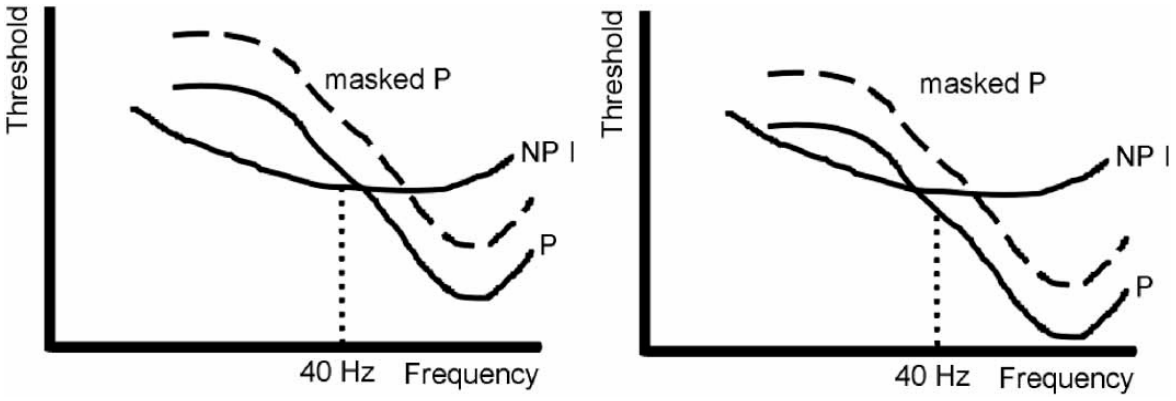

(A) **(B)**

Figure 5.10 The figure shows two possible scenarios regarding the detection of a 40-Hz stimulus by using hypothetical sensitivity curves as a function of stimulus frequency. (A) The threshold of the NP I channel is lower than the threshold of the P channel and the test stimulus is detected by the NP I channel. (B) The threshold of the P channel is lower than the threshold of the NP I channel, so the detection is mediated by the P channel. Note, however, if the P channel is masked (dashed line), the test stimulus is detected by the NP I channel [3].

In Figure 5.10A, or in the first scenario, the detection at 40 Hz is mediated by NP I channel, so that masking the P channel should not have any effect on the thresholds measured at 40 Hz.

However if the situation is like in Figure 5.10B, the second scenario, the unmasked detection at 40 Hz is mediated by P channel. Masking P channel will affect the thresholds at 40 Hz, since by masking the P channel the detection will be mediated by NP I channel which has a higher threshold level than the unmasked P channel.

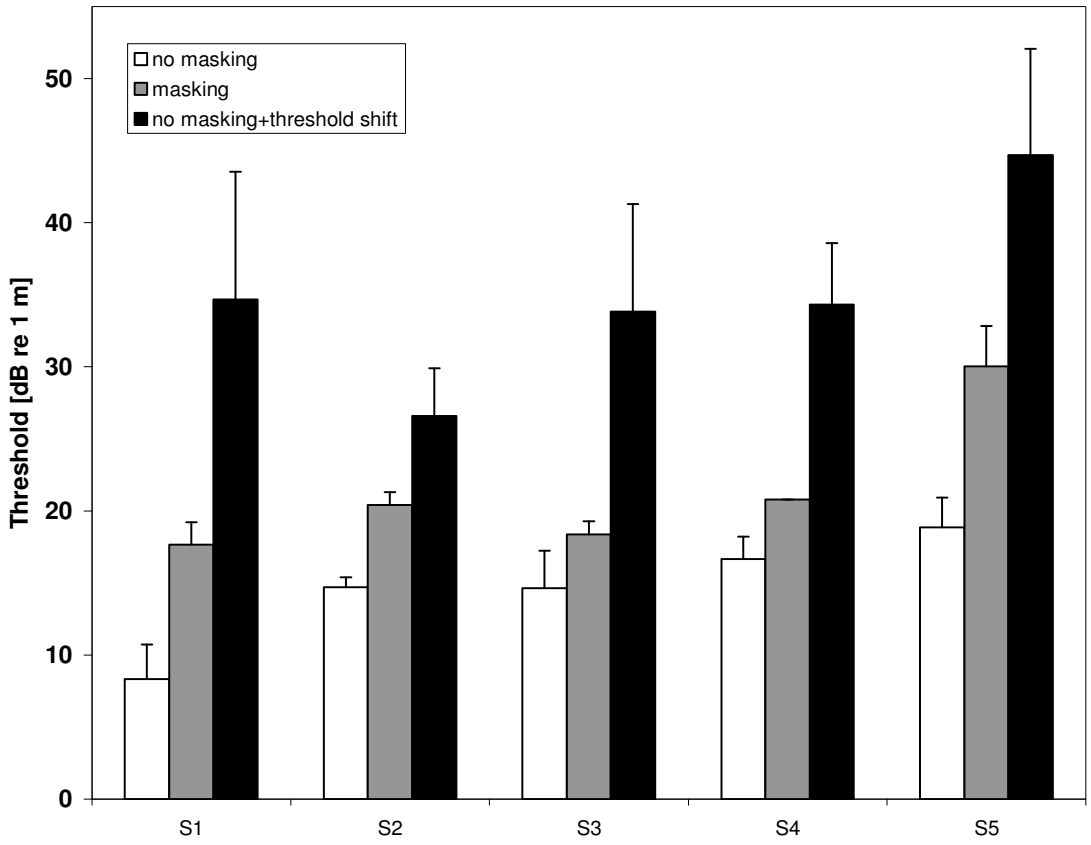

Figure 5.11 White bars show unmasked thresholds at 40 Hz; gray bars show the 40-Hz thresholds obtained using 250-Hz masking. Since gray bars are higher than white bars, the mechanism described in Figure 5.10B is in effect for each subject. The levels of unmasked threshold (white bars) plus the threshold shifts (from Figures 5.5, 5.6, 5.7, 5.8, 5.9) give the predicted thresholds of the masked P channel (black bars). Black bars are higher than gray bars (thresholds of the NP I channel) as expected from the mechanism in Figure 5.10B.

It is not possible to know which of these two scenarios are valid for each subject before testing. Figure 5.11 can help to clarify the situation for each subject.

The white bars are unmasked thresholds at 40 Hz. The gray bars are the 40 Hz thresholds measured by applying a 250 Hz masking stimulus at the sensation levels determined individually for each subjects as mentioned before . The black bars are the summations of unmasked 40 Hz thresholds with the threshold shifts obtained from masking functions of each subject.

As seen from Figure 5.11, gray bars are higher than the white bars which indicates that when the P channel is masked there is always an elevation of threshold at 40 Hz. This

shows that the scenario in Figure 5.10B is valid for each subject and the white bars should be the thresholds of the P channel, and the gray bars are the thresholds of NP I channel at 40 Hz. This hypothesis was tested by the two-sample t-tests.

The black bars are estimates of the masked threshold of the P-channel. If the threshold of P channel is actually raised above the threshold of NP I channel, the black bars are expected to be higher than the gray bars. As Figure 5.11 shows this is the situation. The significance of this effect has been tested by using two-sample t-test. In comparison of white and gray bars statistically, P-values are smaller than 0.001 for S1,S2 and S5; are equal to 0.022, 0.004 for S3 and S4 consecutively. In comparison of gray and black bars statistically, P-values are smaller than 0.001 for all 5 subjects.

Since P values of all tests for each subject is below the significance level of 0.05, it can be understood that the difference between the data represented by the gray and white bars is statistically significant for each subject. There is also a statistical significant difference between gray and black bars.

6. DISCUSSION

The main goal of my study was to find out whether P channel could be masked in order to make the vibrotactile stimuli perceived only by the NP I channel at 40 Hz. The results show that the P channel has lower thresholds than the NP I channel at 40 Hz.

The results further show that the unmasked thresholds are quite similar to the values in the literature.

6.1 Masking Functions

The results of forward-masking experiments show that the four-channel theory can be used to understand the detection mechanism at 40 Hz. By analyzing the experimental data both for unmasked and masked measurements, the threshold levels of the P and NP I channels were determined before and after masking. The results confirm that the masking procedure is reliable and the NP I channel can be selectively activated at 40 Hz. The selectively activation of NP I channel will lead to further studies on investigating NP I channel, such as understanding intensity discrimination in this channel.

The masking functions of my study are in general agreement with the masking functions of Güçlü and Bolanowski's study [3]. Both of these studies used 250 Hz masking and a test stimuli with the same durations. However in Geschedier's [4] study the masking functions are linear (on dB and dB axes) with a slope of 0.70. The slope of the masking function determines the efficiency of masking. These masking functions also had x-intercepts at approximately zero. X-intercept at zero shows that masking intensity at the threshold sensation level produced almost zero threshold shifts in the P channel. The masking functions of my study for each subject shown in Figures 5.5, 5.6, 5.7, 5.8, 5.9 are not consistent with these findings. The masking functions' slopes are 0.6 for S1, 0.06 for S2, 0.15 for S3, 0.29 for S4 and 0.6 for S5. The difference between the slopes of this study and those by Gescheider et al. [4] may be due to the different experimental setups. For example, Gescheider et al. [4] used a test stimulus with a duration of 50 ms which was applied 25 ms after a 700-ms masking stimulus. However, in my study, a test stimulus with

0.5 s duration has followed a 1 s masking stimulus after a 100-ms time gap. This experimental setup difference may have caused different forward masking effect. This could explain the slope differences between this study and Gescheider's [4] study. How can an experimental setup affect slopes' of masking functions cannot be predicted yet. So for different experimental setups, different slopes' can be observed. The masking functions' of this study have linear fit and do not have X-intercepts at zero. If another regression fit is applied, they could have x-intercepts at zero. Other regression fits for masking functions' of this study were not examined. Moreover in this study a contactor surround was not used in order to enable comparisons between psychophysical data and predictions from recent population models of RA fibers as well as current theoretical models cannot include the effects of a surround. It was assumed that the four-channel theory is still valid under this experimental condition. Additionally, with a 0.126 cm^2 contactor, higher masking levels were required to elevate the thresholds of the P channel than the levels reported in the literature. Nevertheless the plots in Figures 5.5, 5.6, 5.7, 5.8, 5.9 signify that each subject may have a different masking function. Since the detection mechanism of 40 Hz stimuli can differ from person to person, for further studies the masking functions for subjects can be different than the masking functions of this study.

7. FUTURE WORK

It is known that the vibrotactile sensitivity decreases with age [18]. A study similar to the study described here can be done on subjects younger or older than the subject group of my study, in order to investigate any changes in masked thresholds and masking functions. The threshold investigation of other Non- Pacinian psychophysical channels can be done without using a contactor surround. Some developmental disorders such as autism and Asperger syndrome can also be the focus of further studies. Additionally my experimental study in tactile thresholds can also be used in studies focusing on auditory and visual thresholds.

REFERENCES

1. Bolanowski, S. J., G.A. Gescheider, R.T.Verrillo, C. M. Checkosky, "Four channels mediate the mechanical aspects of touch", *Journal of the Acoustical Society of America,* Vol. 84, pp. 1680-1694, 1988.

2. Gescheider, G.A., S.J. Bolanowski, K.R. Hardick, "The frequency selectivity of information-processing channels in the tactile sensory system", *Somatosensory and Motor Research*, Vol. 18, pp. 191–201, 2001.

3. Güçlü, B., and S. J. Bolanowski, "Vibrotactile thresholds of the Non-Pacinian I channel", *Somatosensory and Motor Research*, Vol. 22, pp. 49-68, 2005.

4. Gescheider, G.A., M.J. O'Malley, R.T. Verrillo, "Vibrotactile forward masking: Evidence for channel independence", *Journal of the Acoustical Society of America*, Vol. 74, pp. 474–485, 1983.

5. Agache, P. G., C. Monneur, J. L. Leveque, and J. De Rigal, "Mechanical Properties and Young's modulus of human skin in vivo", *Archieve of Dermatological Research,* Vol. 269, pp. 221-232, 1980.

6. Escoffier, C., J. De Rigal, A. Rochefort, R.Vasselet, J. L. Leveque, P. G. Agache, "Age-related mechanical properties of human skin: An in vivo study*", Journal of Investigational Dermatology,* Vol. 93, pp. 353-357*,* 1989.

7. Greenspan, J. D., "A comparison of force and depth of skin indentation upon psychophysical functions of tactile stimuli", *Somatosensory Research,* Vol. 2, pp. 33-48, 1984.

8. Srinavasan, M. A., K. Dandekar, "An investigation of the mechanics of tactile sense using two dimensional models of primate fingertip", *Journal of Biomechanical Engineering,* Vol. 118, pp. 48-55, 1996.

9. Pubols, B. H., “Effect of mechanical stimulus spread across glabrous skin of raccoon and squirrel monkey hand on tactile primary afferent fiber discharge”, *Somatosensory Research*, Vol. 4, pp. 273-308, 1987.

10. Greenspan, J. D., and S.J. Bolanowski, “The psychophysics of tactile perception and its peripheral physiological basis”, In *Handbook of Perception and Cognition 7: Pain and Touch,* L.Kruger, ed., Academic Press, San Diego pp. 25-103, 1996.

11. lifesci.rutgers.edu/~auerbach/bmlec11.pdf

12. Gescheider, G.A., “Psychophysics: The Fundamentals”, Lawrence Erlbaum Associates, Publishers, London, pp. 62-64, 1997.

13. Verrillo, R. T., “Investigation of some parameters of the cutaneous threshold for vibration”, *Journal of the Acoustical Society of America,* Vol. 34, pp. 1768-1773, 1962.

14. Sherrick, C. E., R.W. Cholewiak, and A. A. Collins, “The localization of low-and high frequency vibrotactile stimuli”, *Journal of the Acoustical Society of America,* Vol. 88, pp. 169-179, 1990.

15. Güçlü, B., and S. J. Bolanowski, “Modeling population responses of rapidly-adapting mechanoreceptive fibers”, *Journal of Computational Neuroscience*, Vol. 12, pp. 201-218, 2002.

16. Güçlü, B., and S. J. Bolanowski, “Probability of stimulus detection in a model population of rapidly adapting fibers”, *Neural Computation*, Vol. 16, pp. 39-58, 2004a.

17. Güçlü, B., S. J. Bolanowski, “Tristate Markov model for the firing statistics of rapidly-adapting mechanoreceptive fibers”, *Journal of Computational Neuroscience*, Vol. 17, pp. 107-126, 2004b.

18. Gescheider, G.A., S. J. Bolanowski, K. L. Hall, K. E. Hoffman, R. T.Verrillo, "The effects of aging on information-processing channels in the sense of touch: I. Absolute sensitivity", *Somatosensory and Motor Research*, Vol. 11, pp. 345-357, 1994.

19. Güçlü, B., S. J. Bolanowski, "Time-dependent Markov model for the sinusoidal steady-state response of rapidly-adapting fibers", *Society of Neuroscience* Abstracts 29: Program No.172.16, 2003.

20. Mokous, J. C., G.A. Gescheider, S. J. Bolanowski, "The effects of static indentation on vibrotactile threshold", *Journal of the Acoustical Society of America*, Vol. 99, pp. 3149-3153, 1996.

21. Makous, J.C., G.A. Gescheider, S.J. Bolanowski, "Decay in the effect of vibrotactile masking", *Journal of the Acoustical Society of America*, Vol. 99, pp. 1124–1129, 1996.

22. Zwislocki, J.J., E.M. Relkin, "On a psychophysical transformed rule up and down method converging on a 75% level of correct responses", *PNAS,* Vol. 98, pp. 4811–4814, 2001.